Published in final edited form as:
Clin Cancer Res. 2010 January 1; 16(1): 121–129. doi:10.1158/1078-0432.CCR-09-0982.

Targeting of bone-derived insulin-like growth factor-2 by a human neutralizing antibody suppresses the growth of prostate cancer cells in a human bone environment

Taichi Kimura[1,3], **Takeshi Kuwata**[1], **Satoshi Ashimine**[1,3], **Manabu Yamazaki**[1], **Chisako Yamauchi**[1], **Kanji Nagai**[2], **Akashi Ikehara**[3], **Yang Feng**[4], **Dimiter S. Dimitrov**[4], **Seiichi Saito**[3], and **Atsushi Ochiai**[1]

[1] Pathology Division, Research Center for Innovative Oncology, National Cancer Center Hospital East, Chiba, Japan

[2] Division of Thoracic Oncology, National Cancer Center Hospital East, Chiba, Japan

[3] Division of Urology, Department of Organ-oriented Medicine, Faculty of Medicine, University of the Ryukyus, Okinawa, Japan

[4] Protein Interactions Group, Center for Cancer Research, National Cancer Institute-Frederick, NIH, Frederick, Maryland, USA

Abstract

Purpose—Advanced prostate cancer frequently involves the bone, where the insulin-like growth factor (IGF)-2 is abundant. However, the importance of IGF-2 in bone metastasis from prostate cancer is uncertain. The present study was aimed at examining the therapeutic importance of targeting IGF-2 in bone metastases from prostate cancer.

Experimental design—We investigated whether inhibiting IGF-2 using a human neutralizing antibody (m610) suppresses the growth of prostate cancer cells in a human bone environment. Human MDA PCa 2b prostate cancer cells were inoculated into human adult bone implanted into mammary fat pad of non-obese diabetic/severe combined immunodeficient mice or inoculated into mammary fat pad of the mice without human bone implantation. The mice were treated with m610 or a control antibody (m102.4) once weekly for 4 weeks immediately after inoculation with MDA PCa 2b cells.

Results—Histomorphological examination indicated that m610 treatment significantly decreased the MDA PCa 2b tumor area in the human bone compared with the control. Ki-67 immunostaining revealed that the percentage of proliferating cancer cells in the m610-treated bone tumor sections was significantly lower than that in the control. M610 had no effect on MDA PCa 2b tumor growth

Requests for reprints: Atsushi Ochiai, Pathology Division, Research Center for Innovative Oncology, National Cancer Center Hospital East, 6-5-1, Kashiwanoha, Kashiwa, Chiba 277-8577, Japan. Phone: 81-471-34-6855; Fax: 81-471-34-6865; aochiai@east.ncc.go.jp.

Resident Fellowships from the Foundation for Promotion of Cancer Research in Japan (Taichi Kimura, Satoshi Ashimine, Manabu Yamazaki and Chisako Yamauchi). The Intramural Research Program of the USA NIH, National Cancer Institute, Center for Cancer Research (Yang Feng and Dimiter S. Dimitrov).

Translational relevance

Advanced prostate cancer frequently and organ-specifically metastasizes to the bone. However the efficacy of conventional therapies, including androgen deprivation, for the bone metastasis is unfortunately limited. Thus, more effective treatments are needed. Insulin-like growth factor (IGF)-2 is the most abundant growth factor in human bone. In the present report we highlight the therapeutic impact of IGF-2 in bone metastasis from prostate cancer. Using a human neutralizing antibody against IGF-2 (m610) and a human adult bone implanted mouse-model, we show that inhibiting IGF-2 suppresses the growth of prostate cancer cells in the human bone environment. Our results suggest that targeting of IGF-2 by a neutralizing antibody offers a new therapeutic strategy for bone metastasis from prostate cancer.

in the absence of implanted human bone. M610 prevented the *in vitro* IGF-2-induced proliferation of MDA PCa 2b cells.

Conclusions—Our results indicate that IGF-2 plays an important role in the prostate cancer cell growth in human bone, suggesting that targeting it by neutralizing antibodies offers a new therapeutic strategy for bone metastasis from prostate cancer.

Keywords

Insulin-like growth factor-2; human neutralizing antibody; prostate cancer; bone metastasis; human bone

Introduction

Bone has long been recognized as the most common target organ for prostate cancer metastasis (1,2). Bone metastasis causes skeletal complications and results in poor prostate cancer outcome in patients (3). Unfortunately, the efficacy of conventional therapies, including androgen deprivation, for the bone metastasis is limited. Despite extensive efforts to develop new therapeutic approach, more efficient treatment of bone metastases from prostate cancer has not been established.

Although the precise reason why prostate cancer cells prefer bone tissue is not fully understood, one hypothesis is that the bone is a source of abundant growth factors required for the growth and survival of prostate cancer cells (4). Previously, we established a bone-specific metastasis model of human prostate cancer to investigate the mechanism of bone metastasis from prostate cancer (5). Using this model, in which human adult bones were engrafted in mice, we previously showed that the release of growth factors, such as insulin-like growth factors (IGFs), arising from bone resorption induced by the tumor cells was important for bone metastasis from prostate cancer (6,7).

IGFs are the most abundant growth factors stored in bone matrix (8). The actions of IGFs are inhibited when they bind to IGF-binding proteins. Prostate cancer cells are known to secrete certain IGF-binding protein proteases, as represented by prostate specific antigen (PSA) (9, 10). Thus, the presence of IGF-binding protein proteases could conceivably release IGFs from the complexes, increase the local concentration of free IGFs, which in turn would induce additional growth of prostate cancer cells in the bone microenvironment. In humans, two distinct IGFs are known to exist, IGF-1 and IGF-2. IGF-1 and IGF-2 share a 62% sequence homology and have overlapping but distinct functions: both IGF-1 and IGF-2 activate the IGF-1 receptor (IGF-1R), while IGF-2 also can activate the insulin receptor (IR). Moreover, IGF-2 is the most abundant growth factor in human bone, and the IGF-2 level is 9 times higher than IGF-1 level. In contrast to human bone, IGF-1 is 3 times higher than IGF-2 in mouse bone (11). Interestingly, in our bone transplanted model, human prostate cancer cells metastasized to implanted human bone but not to mouse bone (5). These findings suggest that IGF-2 is more supportive of human prostate cancer than IGF-1 in the human bone environment, which also supports the concept that IGF-2 might be a potentially useful target for the treatment of bone metastases from prostate cancer.

We recently developed a fully human monoclonal antibody (mAb) (m610), which is highly specific for IGF-2 but not for either IGF-1 or insulin (12). To explore the mechanistic role of IGF-2 in the growth of prostate cancer cells in human bone and the therapeutic potential of inhibiting IGF-2 by a neutralizing antibody we used our human adult bone implanted model and a fully human mAb, m610, specific for IGF-2. Our results indicate that IGF-2 plays an important role in the prostate cancer cell growth in human bone and that the human mAb m610

and other anti-IGF-2 mAbs could be promising candidate therapeutics for treatment of prostate cancer.

Materials and Methods

Cell line and cell culture

An androgen-responsive human prostate cancer cell line, MDA PCa 2b, was purchased from the American Tissue Culture Collection (Manassas, VA). The cells were maintained in BRFF-HPC1 medium (Athena Enzyme System, Baltimore, MD) containing 20% FBS and were incubated at 37°C in a humidified atmosphere of 5% CO_2.

Animal care

Male non-obese diabetic/severe combined immunodeficient (NOD/SCID) mice were obtained from CLEA Japan (Tokyo, Japan). The mice were maintained under specific pathogen-free and temperature-controlled air conditions according to Institutional Guidelines. The mice used in the experiments were all 6 to 8 weeks old.

Implantation of human adult bone and induction of bone tumors

After obtaining the informed consent of the patients, human adult bone (HAB) was obtained from lung or esophagus cancer patients (age range, 44 to 82 years; mean, 66.5 years) who had undergone a pulmonary lobectomy or esophagectomy in the Division of Thoracic Oncology, National Cancer Center Hospital East. The implantation of HAB into NOD/SCID mice was performed as previously described, with some modifications (5). Briefly, morselized cancellous bone (200 mm^3) from HAB was implanted into mammary fat pad (MFP) of the mice through a small skin incision in the right flank. In a preliminary examination, graft survival was ascertained by histological examination and the detection of human IgG in the mouse sera using Western blotting at 4 weeks after the implantation. At 4 weeks after bone implantation, single-cell suspensions (8×10^6 cells/100 μL of serum-free medium) of MDA PCa 2b cells were directly injected into the marrow spaces of the implanted HAB.

Induction of MFP tumors

The single-cell suspensions prepared as mentioned above were injected into the MFP of the age-matched NOD/SCID mice (10 to 12 weeks old) through a small skin incision in the right flank.

Human antibodies

An anti-IGF-2 fully human mAb (IgG1 m610), which binds to IGF-2 but not to IGF-1 and insulin, was identified by screening of a large antibody library in the authors' laboratory (National Cancer Institute-Frederick, NIH) (12). To obtain sufficient quantities of m610, m610 was produced from a permanent cell line developed by transfection of CHO-K1 cells and selection of the highest producing clone (13). A control human antibody (IgG1 m102.4), which was produced from a permanent CHO cell line under the same conditions as m610 (14), was chosen to be as closed in sequence as possible to m610 but with entirely different specificity. Compared to m610, m102.4 has identical Fc, hinge and CH1, very similar CL and similar frameworks of the variable domains but different complementarity-determining regions to ensure specificity to Hendra and Nipah virus.

Protocol for m610 treatment

In the model involving the induction of bone tumor in HAB (HAB model), m610 (1 or 10 mg/kg) or a control antibody (10 mg/kg) (n = 8 per each group) was intraperitoneally administered to the mice at weekly intervals for 4 weeks starting immediately after the inoculation of the

MDA PCa 2b cells into the HAB. In the model involving the induction of tumors in MFP (MFP model), m610 (10 mg/kg) or control antibody (10 mg/kg) (n = 5 or 4 per group, respectively) was administered to the mice at weekly intervals for 4 weeks after the inoculation of the cells into the MFP. At 4 weeks after the start of the m610 treatment, the mice were sacrificed and the HAB tissues and mouse organs (lung, liver, spleen, kidney, lumbar vertebrae) in the HAB model and the MFP tissues in the MFP model were harvested. The body weight of mouse was measured at the time of HAB implantation, the start of the m610 treatment and the time of sacrifice.

Histomorphometric examination

Harvested specimens were fixed in 10% neutral buffered formalin and embedded in paraffin. The bone specimens were decalcified with EDTA solution (Wako, Osaka, Japan) before paraffin embedding. Two-μm-thick sections were prepared from each specimen. Then, we analyzed the tumor burden in the HAB and the MFP by histomorphometrically examining sections stained for PSA, as described previously (6). Briefly, tissue sections of the HAB and MFP specimens were cut at three levels far enough apart (> 200 μm) to avoid replicating the sampling of a single surface event; immunostaining for PSA was performed using the EnVision Plus System HRP kit (Dako, Glostrup, Denmark) according to the manufacturer's protocol. An anti-PSA polyclonal antibody (1:800; Dako) was used as a primary antibody. Antigen retrieval was not performed. The total tissue area and the total tumor area immunostained by the anti-PSA antibody were determined using image-analysis software (Image J version 1.38x, National Institutes of Health, Bethesda, MD). The results were expressed as the absolute tumor area (mm^2) and the tumor area as a percentage of the tissue section area (%).

Immunohistological examination

The immunostaining procedure used for IGF-1R, IR, Ki-67 and cleaved caspase-3 was the same as described above. However, microwaving (95°C, 20 min) in citrate buffer (pH 6.0) or in Target Retrieval Solution High pH buffer (Dako) was required for Ki-67 antigen retrieval or cleaved caspase-3 antigen retrieval, respectively. An anti-IGF-1R mAb (1:100; Chemicon, Temecula, CA), an anti-IR mAb (1:100; Chemicon), an anti-Ki-67 mAb (1:50; Dako) or an anti-cleaved caspase-3 polyclonal antibody (1:200; Cell Signaling Technology, Beverly, MA) was used as a primary antibody.

To evaluate the proliferative and apoptotic statuses of the tumor cells, we counted the number of Ki-67-positive and cleaved caspase-3-positive cancer cells and the total cancer cells in three high power fields of the most strongly stained tumor areas and then calculated the percentages of these immunostaining positive cancer cells to the total cells. The necrotic area was not included in the evaluation of apoptosis. The data from samples with the presence of cancer cells were presented.

Determination of serum PSA levels

Blood samples were obtained from the mice before sacrifice. The serum PSA levels were determined using a chemiluminescent enzyme immunoassay kit (Hybritech-PSA, Beckman Coulter, San Diego, CA) according to the manufacturer's protocol.

Proliferation assay

MDA PCa 2b cells (5×10^5) seeded on a 3.5-cm dish were cultured in complete growth medium for 48 hours to allow cell adhesion. After changing the medium to serum-free F12K medium (Invitrogen, Carlsbad, CA, USA), the cells were treated for 48 hours with serum-free medium alone, with recombinant human IGF-2 (1, 10 or 100 ng/mL, R&D Systems, Minneapolis, MN), with the control antibody (10 μg/mL) plus IGF-2 (100 ng/mL), with m610 (0.1, 1 or 10 μg/

mL) plus IGF-2 (100 ng/mL), or with m610 (10 μg/mL) in the absence of IGF-2. The cells were dislodged by trypsinization and the number of viable cells was counted using the trypan blue (Invitrogen) exclusion assay.

Phosphorylation assay

MDA Pca 2b cells (4×10^6) seeded on a 6-cm dish were cultured in complete growth medium for 48 hours. The cells were rinsed and cultured in serum-free F12K for 6 hours. Then the cells were treated with the serum-free medium alone, with IGF-1 (100 ng/ml, R&D systems), or with IGF-2 (100 ng/ml) for 15 minutes. Immunoprecipitation and western blot analysis procedures were performed as described previously (15). Two hundred micrograms of protein from each cell lysate were respectively immunoprecipitated with an anti-IGF-1R polyclonal antibody (2 μg; clone C-20; Santa Cruz Biotechnology, Santa Cruz, CA) or with an anti-IR polyclonal antibody (2 μg; clone C-19; Santa Cruz Biotechnology) for 12 hours at 4°C, and the each immunoprecipitate was collected using protein G Sepharose. Each sample (derived from 20 μg total cell lysate) was fractionated by 7.5% SDS-PAGE and transferred to PVDF membrane (Millipore, Bedford, MA). The membranes were probed with an anti-phosphotyrosine mAb (1:2000; clone 4G10; Upstate Biotechnology, Lake Placid, NY) and visualized by an enhanced chemiluminescence (Amersham Biosciences, Piscataway, NJ). After stripping the membrane, total IGF-1R or IR in the immunoprecipitates was detected with C-20 antibody or C-19, respectively.

In an assay for the effect of IGF-2 on phosphorylation of Akt and MAPK, the cells were treated with the serum-free medium or with IGF-2 (1, 10 or 100 ng/ml) for 15 minutes. In an assay for the inhibitory effect of m610 on the IGF-2-induced phosphorylation of IGF-1R, IR and Akt, the cells were pre-incubated for 30 minutes with m610 (0.1, 1 or 10 μg/ml) prior to IGF-2-treatment (100 ng/ml). Twenty-microgram proteins from the lysates were subjected to a western blot analysis. To detect phosphorylated IGF-1R and IR, a polyclonal antibody specific for both phosphorylated tyrosine 1135/1136 of IGF-IRβ and phosphorylated tyrosine 1162/1163 of IRβ was used (1:1000; BioSource International, Camarillo, CA). Phospho-Akt, total-Akt, phospho-MAPK or total MAPK was respectively detected with an anti-phospho-Akt (Serine 473) polyclonal antibody, an anti-Akt polyclonal antibody, an anti-phospho-MAPK (Tyrosine 202/204) mAb or an anti-MAPK polyclonal antibody (1:1000 each; Cell Signaling Technology, Beverly, MA).

Statistical analysis

Data are expressed as the mean ± SE. Variables were compared between the experimental and control groups using a Student's *t*-test. The relation between the percentage of the tumor area and the serum PSA level was assessed using a linear regression analysis. Statistical calculations were performed on a Windows personal computer with the GraphPad PRISM software, version 4.03 (GraphPad Software, San Diego, CA). A value of $P < 0.05$ was considered statistically significant.

Results

Effect of m610 on the growth of bone tumors from MDA PCa 2b cells in HAB

To investigate the effect of m610 on the growth of bone tumors from prostate cancer cells in human bone tissue, m610 (low dose, 1 mg/kg; high dose, 10 mg/kg) or control antibody (10 mg/kg) was administered to the mice with HAB implantation according to the protocol (Fig. 1). At 4 weeks after the treatments, a histomorphological analysis of the HAB specimens was performed. All 8 of the control antibody-treated mice, 7 of the 8 mice in the low-dose group and 6 of the 8 mice in the high-dose group developed bone tumors. The mean total tumor areas in the low-dose and high-dose groups were 0.8 ± 1.5 and 0.8 ± 1.2 mm^2, respectively; these

values were significantly smaller than that in the control group (2.2 ± 0.9 mm^2; P = 0.0397, P = 0.0152, respectively; Fig. 2A and B). The mean percentages of the tumor area to the total tissue section area in the low-dose and high-dose groups were 0.7% ± 1.4% and 0.6% ± 0.9%; these values were also significantly lower than that in the control (2% ± 0.8%; P = 0.0438, P = 0.0075, respectively; Fig. 2C).

To further assess the effect of m610 on tumor growth, serum PSA level, which is widely used for the diagnosis and therapeutic evaluation of prostate cancer, was measured. The serum PSA levels of the m610-treated groups were significantly lower than that of the control group, in parallel with the reduction in the tumor area (low-dose group: P = 0.0384, high-dose group: P = 0.0072, Fig. 2D). Additionally, a strong correlation was observed between the percentage of the tumor area and the serum PSA values (r^2 = 0.7656, P < 0.0001, linear regression analysis).

Together, these results of the histomorphological examination and the PSA measurement demonstrate that m610 significantly suppressed the growth of bone tumors induced by MDA PCa 2b cells in implanted HAB, although a dose escalation effect of m610 on the response was not observed.

Immunohistological examination of m610-treated bone tumor sections in the HAB model

To understand the processes by which the bone tumor growth was suppressed by m610, immunohistological examinations were performed. First, we examined the expression levels of IGF-1R and IR, which are functional receptors of IGF-2, on the bone tumors by MDA PCa 2b cells in HAB. IGF-1R and IR were diffusely expressed in both the control and m610-treated bone tumors (Fig. 3A and B), and no differences in the expression levels of these receptors were microscopically observed between the bone tumors. These findings indicate that the suppressive effect of m610 on the bone tumor growth was not caused by alterations in the expression levels of these receptors. Next, immunohistological staining for Ki-67 or cleaved caspase-3 was performed to investigate the proliferative and apoptotic statuses of the bone tumors. Compared with the control, an apparent decrease in the number of cancer cells with Ki-67-positive nuclei was observed in the m610-treated bone tumor sections (Fig. 4A), while a slightly increased number of cleaved caspase-3-positively stained cancer cells was observed (Fig. 4B). Then, the percentages of positively immunostained cancer cells out of the total cell numbers were calculated in three high power fields with the most highly stained tumor areas. As shown in Fig. 4C, the percentages of Ki-67-positive cancer cells in the m610-treated groups were significantly lower than that in the control (low-dose group: P = 0.0007, high-dose group: P = 0.0002). Meanwhile, the mean percentages of cleaved caspase-3-positive cancer cells in the m610-treated groups were slightly higher than that in the control, but not significantly (Fig. 4D; low-dose group: P=0.1937, high-dose group: P=0.0601). These findings show that m610 suppressed the proliferation of MDA PCa 2b cells in HAB, but did not lead to a significant increase of apoptosis although a trend to an increase was observed for the high dose group.

Effect of m610 on the growth of tumors from MDA PCa 2b cells in MFP

To examine whether m610 exerts a direct growth-inhibitory effect on MDA PCa 2b cells, m610 (10 mg/kg) or control antibody (10 mg/kg) was administered to the mice without HAB implantation according to the protocol (Fig. 1). Three of the 4 control antibody-treated mice and 4 of the 5 m610-treated mice developed tumors in the MFP tissue. The mean total tumor areas of the control and m610-treated tumors in the MFP model were 1.1 ± 1.5 mm^2 and 1.3 ± 1.4 mm^2, respectively (P = 0.8787) (Fig. 5A). The mean percentages of the tumor area to the total tissue section area in the control and m610-treated group were 1.3% ± 1.8% and 2% ± 2.1%, respectively (P = 0.6332). The serum PSA levels of the control and m610-treated group were 0.6±0.9 and 2.7±1.2 ng/ml, respectively (P = 0.2912). An immunohistological examination revealed that IGF-1R and IR were focally expressed on both the control and m610-

treated tumors in the MFP tissue and that the expression levels of the receptors were not different between the tumors (Supplemental. Fig. 1A and B). Ki-67 immunostaining revealed that the proliferative statuses were similar between the control and m610-treated tumors, consistent with the results for tumor size (Supplemental. Fig. 1C, Fig. 5B; P = 0.7462). Together, these findings indicate that m610 had no effect on the growth of MDA PCa 2b cells in MFP, unlike in HAB, demonstrating that the inhibitory effect of m610 on tumor cell proliferation is restricted to within the bone.

Inhibition of IGF-2-induced cell proliferation and signaling in MDA PCa 2b cells by m610

Using a cell proliferation assay, we confirmed that m610 inhibits the IGF-2-induced proliferation of MDA PCa 2b cells. Exogenous IGF-2 dose-dependently induced the proliferation of MDA PCa 2b cells (Fig. 6A, lanes 1–4). The control antibody had no inhibitory effect on the IGF-2-induced cell proliferation (Fig. 6A, lane 5). M610 at doses of 1 and 10 μg/mL significantly inhibited the IGF-2-induced cell proliferation, compared with the control antibody group (Fig. 6A, lanes 7 and 8; P=0.0049, 0.0039, respectively). But m610 had no effect on the proliferation of MDA PCa 2b cells without exogenous IGF-2-stimulation, indicating that m610 did not have a direct effect on the cells (Fig. 6A, lane 9).

To confirm that m610 prevents signal transduction mediated by receptor interaction with IGF-2 in MDA PCa 2b cells, we firstly investigated whether IGF-2 activates IGF-1R and IR in the cells by immunoprecipitation-western blot analysis. Upon ligand binding, IGF-1R and IR undergoes autophosphorylation of tyrosine residues in their β-subunits. The western blot analysis showed that IGF-2 induces phosphorylation of tyrosines in each receptor in MDA PCa 2b cells (Fig. 6B). Note that IGF-2 induces significantly higher level of IR phosphorylation than of the IGF-1R phosphorylation. In contrast, IGF-1 induces much higher levels of phosporylation of the IGF-1R than of the IR. Tyrosine phosphorylation of IGF-1R or IR leads to phosphorylation of the downstream kinases Akt and MAPK. We next examined whether IGF-2 induces the downstream kinases in MDA PCa 2b cells by a western blot analysis. IGF-2 induced Akt phosphorylation in the cells, but not MAPK phosphorylation (Supplemental Fig. 2). We finally investigated whether m610 prevents the IGF-2-induced IGF-1R and IR signaling in MDA PCa 2b cells by a western blot analysis. To detect the total amount of activated statuses (IGF-1R plus IR) which is most relevant for the degree of induced cell proliferation, an antibody specific for phosphorylated tyrosines of IGF-1R and IR was used in the analysis. As shown in Fig. 6C, the m610 dose-dependently prevented the IGF-2-induced tyrosine phosphorylation of IGF-1R/IR as well as serine phosphorylation of Akt in MDA PCa 2b cells.

Discussion

IGF-2 is the most abundant growth factor in human bone (8) and, unlike in mouse bone, is 9 times more abundant than IGF-1 (11). Our previous study revealed the role of IGFs in prostate cancer growth in human bone, as shown by the suppressive effect of a neutralizing antibody (KM1468), which cross-reacts with human IGF-1 and IGF-2 and mouse IGF-2, on the growth of MDA PCa 2b cells in implanted HAB (6). Moreover, another study of ours indicated that tail vein-injected prostate cancer cells preferentially metastasized to implanted HAB, rather than to implanted mouse bone or native bone (5). These findings suggested that IGF-2 may support human prostate cancer more efficiently than IGF-1 in human bone environment, in accordance with the “seed and soil” theory by Paget (16) for metastasis. Therefore, we became interested in specifically targeting IGF-2 as a potential therapy for bone metastasis from prostate cancer.

Although clinical studies have suggested that IGF-2 contributes to the development and progression of several cancers including prostate cancer (17–19), only a few studies by others and us have reported an *in vivo* antitumor effect of targeting IGF-2. O’Gorman et al. reported

that the overexpression of the IGF-2 receptor, which is a clearance receptor for IGF-2, on choriocarcinoma cells reduced the cell growth *in vitro* and *in vivo*, indicating that inhibiting IGF-2 is a potential target for cancer therapy (20). In an another strategy using neutralizing antibodies, Miyamoto et al. reported that an IGF-2 neutralizing antibody partly suppressed the development of liver metastasis induced by the intrasplenic injection of colon cancer cells, whereas IGF-1 neutralizing antibody significantly suppressed the development of liver metastasis (21). Because IGF-2 production in rodents becomes attenuated in most tissues soon after birth unlike IGF-1 production (22), the effect of IGF-2 as an endocrine and/or paracrine on tumor growth may be underestimated in models using mouse-native organs.

The present study demonstrated that inhibiting IGF-2 by m610 effectively suppresses the growth of prostate cancer cells in a human bone environment. The following results support this conclusion: (a) m610 significantly suppressed the growth of bone tumors from MDA PCa2b cells in implanted HAB; it even decreased the number of mice developing tumors from 8 to 6 although larger number of mice are needed to confirm this effect; (b) Ki-67 immunostaining revealed that the proliferative status of m610-treated bone tumor was apparently suppressed; (c) in the absence of HAB, m610 had no effect on the growth of tumors from MDA PCa 2b cells, indicating that the suppressive effect of m610 on the tumor cells was restricted to those within HAB; and (d) *in vitro* assays confirmed that m610 prevents the exogenous IGF-2-induced proliferation of MDA PCa 2b cells. These results provide clear evidence of the important role of IGF-2 for tumor growth in the HAB model and of an *in vivo* antitumor effect of m610 on metastatic bone tumor from prostate cancer through a mechanism involving the inhibition of IGF-2. They also underscore the notion that IGF-2 levels in local tissue may be more relevant in tumor promotion than its plasma levels, and that a paracrine mechanism of IGF-2 may play a critical role in tumor growth.

The potency of m610 on the growth inhibition of MDA PCa 2b cells in the HAB model is 65% whereas that of the previously published antibody, KM1468 is 97%, compared to the respective controls: the antitumor effect of inhibiting IGF-2 alone is lower than that of inhibiting both IGF-1 and IGF-2 in the HAB model. Despite the lower antitumor effect of m610 in the HAB model, targeting IGF-2 by m610 might provide certain clinical benefits in cancer therapy for the following reasons. a) Growth hormone (GH) feedback is not known for IGF-2, but IGF-1 is regulated by this feedback. Lowering IGF-1 concentration triggers feedback upregulation of the GH; the GH compensates for the reduced IGF-1 levels. Thus, targeting IGF-1 might require high concentrations of anti-IGF-1 antibodies. It should be noted that KM1468 is not reactive with mouse IGF-1 and therefore its use in our HAB model does not trigger the GH feedback on the IGF-1 and the tumor growth. b) Because m610 is a fully human antibody, its clinical use is less likely to induce immune reactions compared to murine antibodies.

Targeting IGF-2 might provide additional therapeutic benefit in combination with other treatments. IGF-1R activation by IGF-1 and IGF-2 has been shown to stimulate the growth of a wide range of cancer cells (23,24). Currently, potent mAbs against the IGF-1R are being tested in clinical trials against multiple tumor types including prostate, breast and colon cancers, and Ewing's sarcoma (25). Importantly, it is becoming increasingly evident that IR activation by IGF-2 enhances the growth of Ewing sarcoma and breast cancer in addition to the IGF-1R activation: cotargeting IGF-1R and IR is likely to be more effective than targeting the IGF-1R alone (26–28). Recently reported immunohistological examinations of primary human prostate cancer show that IGF-1R as well as IR are both commonly expressed on the tissues (29). Our results from the immunohistological examinations (Figure 3) and Western blot analyses (Figure. 6B and C) suggest that IR activation by IGF-2 plays an important role in the prostate cancer cell growth in bone in addition to the IGF-1R activation. Based on these findings, IGF-2 could be a promising candidate target in therapeutic strategies for cotargeting IGF-1R and IR.

If m610 were capable of suppressing the growth of prostate cancer in bone without any adverse reactions, m610 therapy might considerably improve the quality of life of patients with bone metastases of prostate cancer. In the present study, the administration of m610 did not affect the body weights of mice during the 4-week treatment period (Supplemental. fig. 3), and no adverse findings were observed in the histological examination for the mouse organs.

In conclusion, the present study demonstrated that an IGF-2-specific antibody, m610, can sufficiently suppress the growth of bone tumors from MDA PCa 2b cells in a human bone environment and that this effect is caused by the suppression of the tumor cells' proliferative status. These results suggest that the targeting of bone-derived IGF-2 using a neutralizing antibody offer a new therapeutic strategy for bone metastasis from prostate cancer.

Supplementary Material

Refer to Web version on PubMed Central for supplementary material.

Acknowledgments

We thank Sachiko Fukuda and Hiroko Hashimoto for technical assistance, Motoko Suzaki for secretarial support, and Maki Touko, Hiroyuki Maeda, Takako M. Oki and Hiroyuki Yonou for their suggestions.

Grant support: Grant-in-Aid for the Third-Term Comprehensive 10-Year Strategy for Cancer Control from the Ministry of Health and Welfare of Japan and Research

References

1. Abrams HL, Spiro R, Goldstein N. Metastasis in carcinoma: analysis of 1000 autopsied cases. Cancer (Phila) 1950;3:74–85. [PubMed: 15405683]
2. Bubendorf L, Schopfer A, Wagner U, et al. Metastatic patterns of prostate cancer: an autopsy study of 1,589 patients. Hum Pathol 2000;31:578–83. [PubMed: 10836297]
3. Soloway MS. The importance of prognostic factors in advanced prostate cancer. Cancer 1990;66:1017–21. [PubMed: 2393845]
4. Yoneda T. Cellular and molecular mechanisms of breast and prostate cancer metastasis to bone. Eur J Cancer 1998;34:240–5. [PubMed: 9741327]
5. Yonou H, Yokose T, Kamijo T, et al. Establishment of a novel species- and tissue-specific metastasis model of human prostate cancer in humanized non-obese diabetic/severe combined immunodeficient mice engrafted with human adult lung and bone. Cancer Res 2001;61:2177–82. [PubMed: 11280783]
6. Goya M, Miyamoto S, Ohki Y, et al. Growth inhibition of human prostate cancer cells in human adult bone implanted into non-obese diabetic/severe combined immunodeficient mice by a ligand-specific antibody to human insulin-like growth factors. Cancer Res 2004;64:6252–8. [PubMed: 15342412]
7. Yonou H, Kanomata N, Goya M, et al. Osteoprotegerin/osteoclastogenesis inhibitory factor decreases human prostate cancer burden in human adult bone implanted into nonobese diabetic/severe combined immunodeficient mice. Cancer Res 2003;63:2096–102. [PubMed: 12727825]
8. Hauschka PV, Mavrakos AE, Iafrati MD, Doleman SE, Klagsbrum M. Growth factors in bone matrix. Isolation of multiple types by affinity chromatography on heparin-sepharose. J Biol Chem 1986;261:12665–74. [PubMed: 3745206]
9. Rehault S, Monget P, Mazerbourg S, et al. Insulin-like growth factor binding proteins (IGFBPs) as potential physiological substrates for human kallikreins hK2 and hK3. Eur J Biochem 2001;268:2960–8. [PubMed: 11358513]
10. Maeda H, Yonou H, Yano K, Ishii G, Saito S, Ochiai A. Prostate-specific antigen enhances bioavailability of insulin-like growth factor by degrading insulin-like growth factor binding protein 5. Biochem Biophys Res Commun 2009;381:311–6. [PubMed: 19250630]
11. Bautista CM, Mohan S, Baylink DJ. Insulin- like growth factors I and II are present in the skeletal tissues of ten vertebrates. Metabolism 1990;39:96–100. [PubMed: 2104643]

12. Feng Y, Zhu Z, Xiao X, Choudhry V, Barrett JC, Dimitrov DS. Novel human monoclonal antibodies to insulin-like growth factor (IGF)-II that potently inhibit the IGF receptor type I signal transduction function. Mol Cancer Ther 2006;5:114–20. [PubMed: 16432169]
13. Feng Y, Dimitrov DS. Scaling up and production of therapeutic antibodies for preclinical studies. Methods Mol Biol 2009;525:499–508. [PubMed: 19252843]
14. Zhu Z, Bossart KN, Bishop KA, et al. Exceptionally potent cross-reactive neutralization of Nipah and Hendra viruses by a human monoclonal antibody. J Infect Dis 2008;197:846–53. [PubMed: 18271743]
15. Miyamoto S, Yano K, Sugimoto S, et al. Matrix metalloprotease-7 facilitates insulin-like growth factor bioavailability through its proteinase activity on insulin-like growth factor binding protein-3. Cancer Res 2004;64:665–71. [PubMed: 14744783]
16. Paget S. The distribution of secondary growths in cancer of the breast. Lancet 1889;1:571–3.
17. Fürstenberger G, Senn HJ. Insulin-like growth factors and cancer. Lancet Oncol 2002;3:298–302. [PubMed: 12067807]
18. Trojan L, Bode C, Weiss C, et al. IGF-II serum levels increase discrimination between benign prostatic hyperplasia and prostate cancer and improve the predictive value of PSA in clinical staging. Eur Urol 2006;49:286–92. [PubMed: 16386354]
19. Cardillo MR, Monti S, Silverio FD, Gentile V, Sciarra F, Toscano V. Insulin-like growth factor (IGF)-I, IGF- II and IGF type I receptor (IGFR-1) expression in prostatic cancer. Anticancer Res 2003;23:3825–36. [PubMed: 14666684]
20. O'Gorman DB, Weiss J, Hettiaratchi A, Firth SM, Scott CD. Insulin-like growth factor-II/mannose 6-phosphate receptor overexpression reduces growth of choriocarcinoma cells in vitro and in vivo. Endocrinology 2002;143:4287–94. [PubMed: 12399424]
21. Miyamoto S, Nakamura M, Shitara K, et al. Blockade of paracrine supply of insulin-like growth factors using neutralizing antibodies suppresses the liver metastasis of human colorectal cancers. Clin Cancer Res 2005;11:3494–502. [PubMed: 15867252]
22. Sussenbach JS, Steenbergh PH, Holthuizen P. Structure and expression of the human insulin-like growth factor genes. Growth Regul 1992;2:1–9. [PubMed: 1486331]
23. Baserga R. Targeting the IGF-1 receptor: from rags to riches. Eur J Cancer 2004;40:2013–5. [PubMed: 15341972]
24. Bohula EA, Playford MP, Macaulay VM. Targeting the type 1 insulin like growth factor receptor as anti-cancer treatment. Anticancer Drugs 2003;14:669–82. [PubMed: 14551500]
25. Pollak M. Insulin and insulin-like growth factor signaling in neoplasia. Nat Rev Cancer 2008;8:915–28. [PubMed: 19029956]
26. Sciacca L, Costantino A, Pandini G, et al. Insulin receptor activation by IGF-II in breast cancers: evidence for a new autocrine/paracrine mechanism. Oncogene 1999;18:2471–9. [PubMed: 10229198]
27. Sachdev D, Yee D. Disrupting insulin-like growth factor signaling as a potential cancer therapy. Mol Cancer Ther 2007;6:1–12. [PubMed: 17237261]
28. Avnet S, Sciacca L, Salerno M, et al. Insulin receptor isoform A and insulin-like growth factor II as additional treatment targets in human osteosarcoma. Cancer Res 2009;69:2443–52. [PubMed: 19258511]
29. Cox ME, Gleave ME, Zakikhani M, et al. Insulin receptor expression by human prostate cancers. Prostate 2009;69:33–40. [PubMed: 18785179]

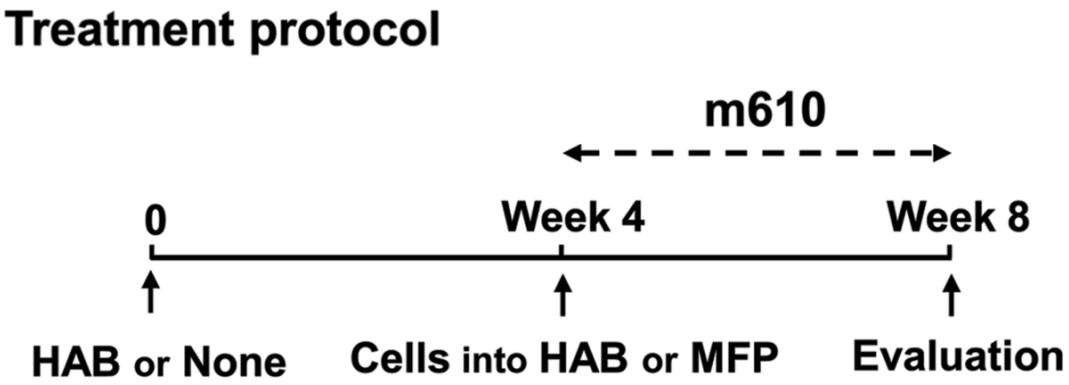

Fig. 1. Summary of treatment protocol

On day 0, NOD/SCID mice were either implanted with HAB into MFP tissues or not. After 4 weeks, MDA PCa 2b cells were inoculated into the implanted HAB or into MFP tissues of the mice without implantation. Weekly administration of m610 was started immediately after the cell inoculation. At 4 weeks after the treatment, the mice were sacrificed for histological analysis and measurement of serum PSA.

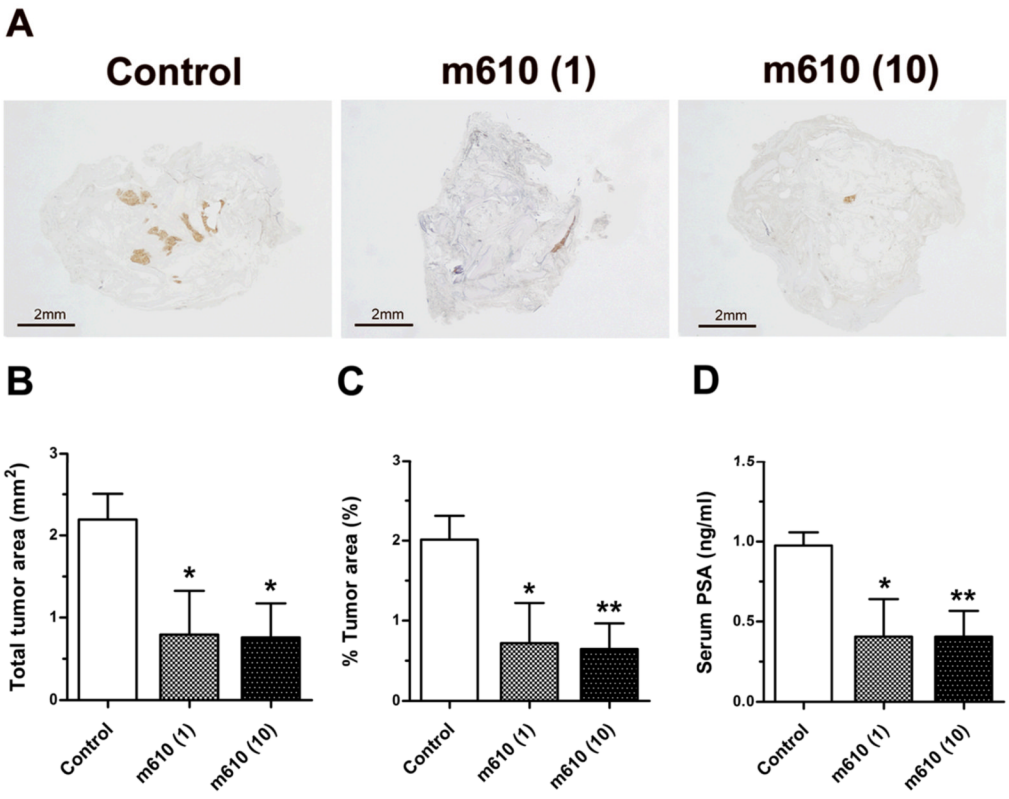

Fig. 2. M610 suppresses the growth of bone tumors from MDA PCa 2b cells in HAB

A representatively shows macroscopic images of the PSA-stained HAB sections from control and m610-treated groups. Localized PSA-positive MDA PCa 2b tumor foci were observed. Scale bars, 2 mm. The sections were histomorphologically analyzed for **B**, total tumor area and **C**, percentage of tumor area to total HAB tissue area. **D**, serum PSA values in blood samples of the groups. Control; control antibody group, m610 (1); low-dose (1 mg/kg) group, m610 (10); high-dose (10 mg/kg) group. Data are the means for 8 mice in each group; bars, ± SE. *P<0.05; **P<0.01, compared with the control.

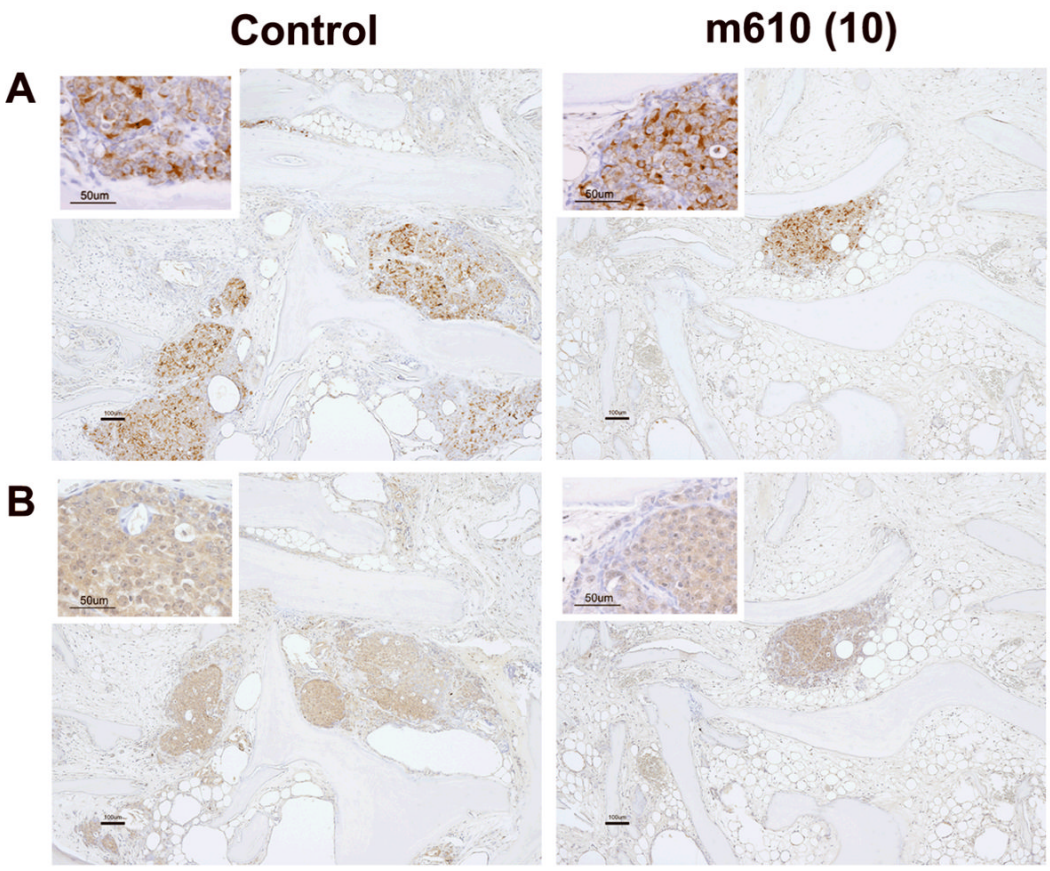

Fig. 3. IGF-1R and IR are expressed in MDA PCa 2b tumors in HAB

A, IGF-1R immunostained images of HAB sections from control and high-dose group are representatively shown. **B,** IR immunostained images. Scale bars, 100 μm. The higher magnification insets show the tumor cells with membranous and cytoplasmic immunostaining for IGF-1R and IR, respectively (Scale bars, 50 μm).

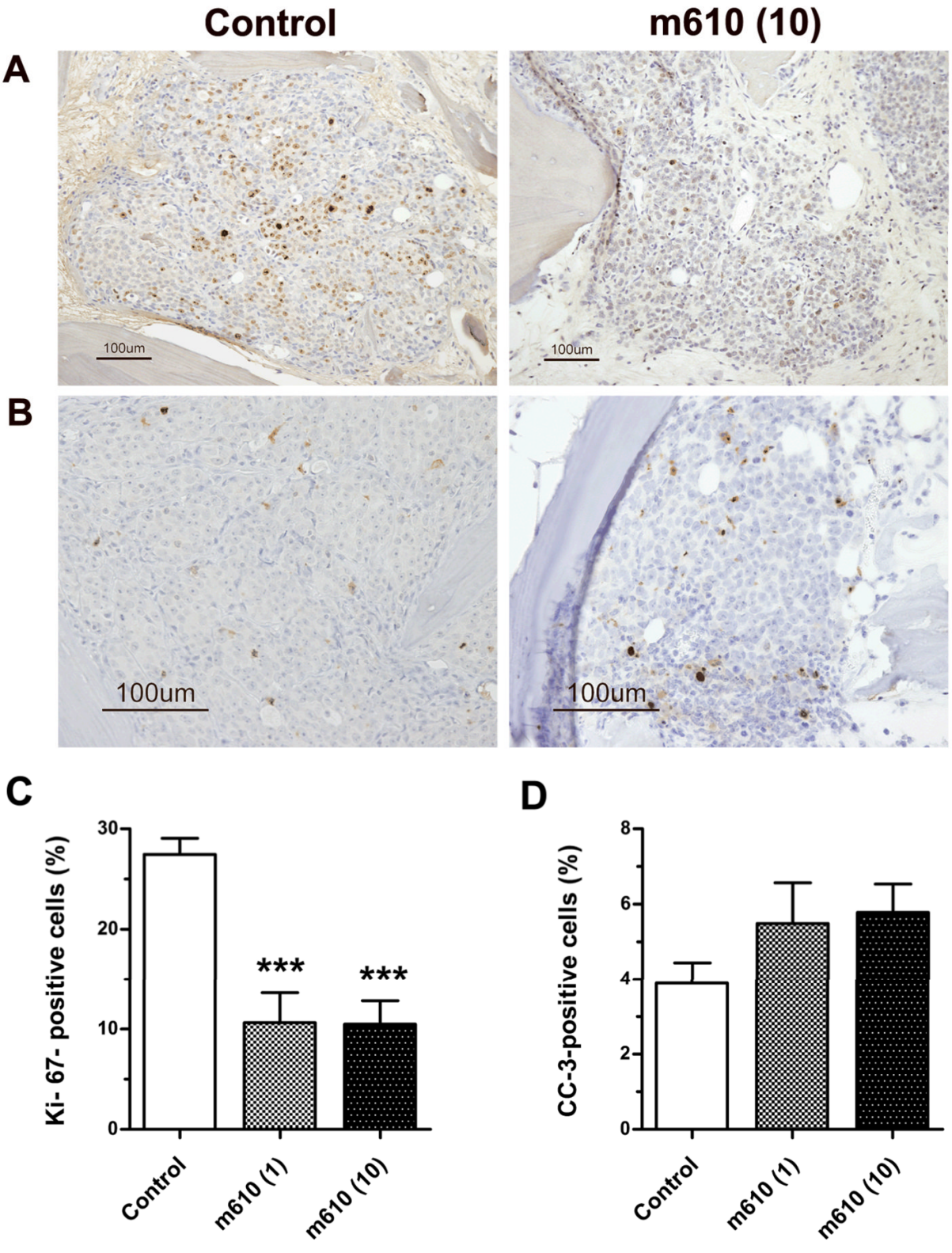

Fig. 4. M610 suppresses the proliferative status of MDA PCa 2b tumors in HAB

A, Ki-67 immunostained images of HAB sections from control and high-dose group are representatively shown. **B,** cleaved caspase-3 immunostained images. Scale bars, 100 μm. The percentages of positively immunostained cancer cells to the total cells were calculated. **C** and **D**, percentages of Ki-67-positive and cleaved caspase-3-positive cancer cells, respectively. CC-3, cleaved caspase-3. Data are the means; bars, ± SE. ***P < 0.001, compared with the control.

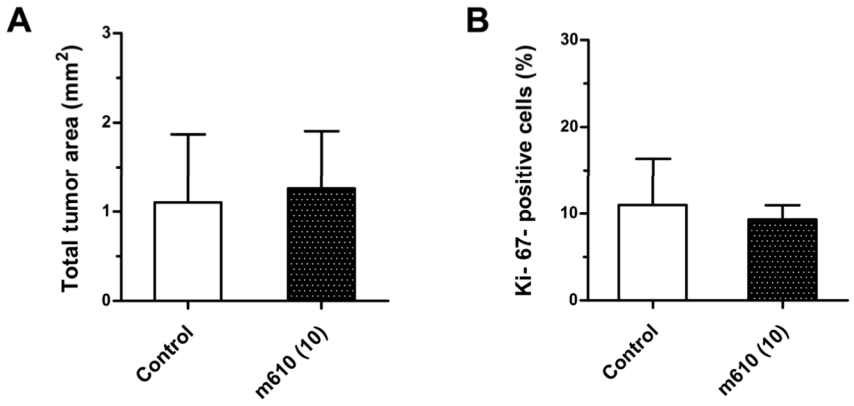

Figure 5. M610 does not suppress the growth of tumors from MDA PCa 2b cells in MFP

Histological analyses in MFP model. **A**, total tumor area. The data are the means for 4 mice in the control group and 5 mice in the m610-treated group; bars, ± SE. **B**, percentages of Ki-67-positive cancer cells.

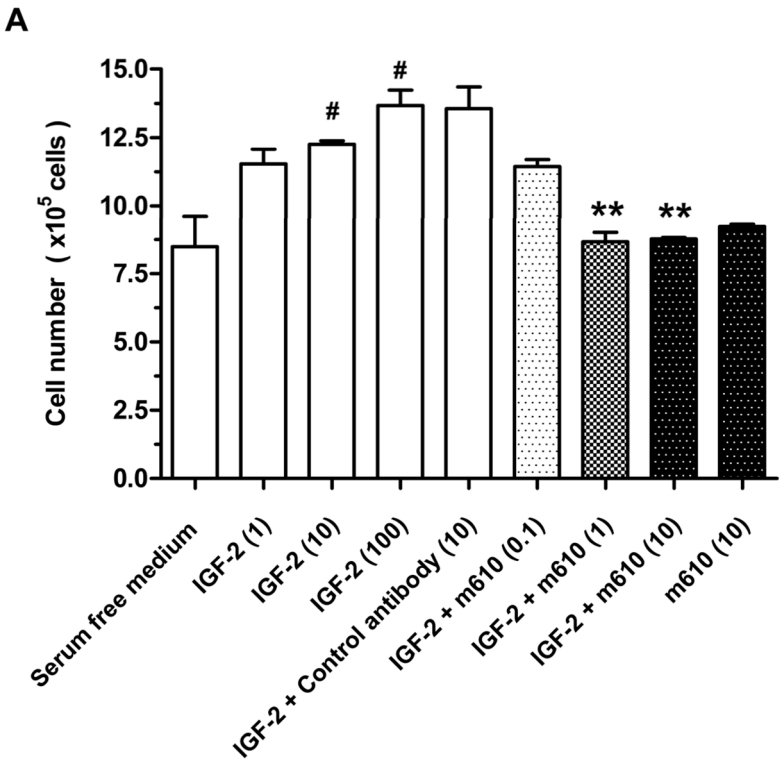

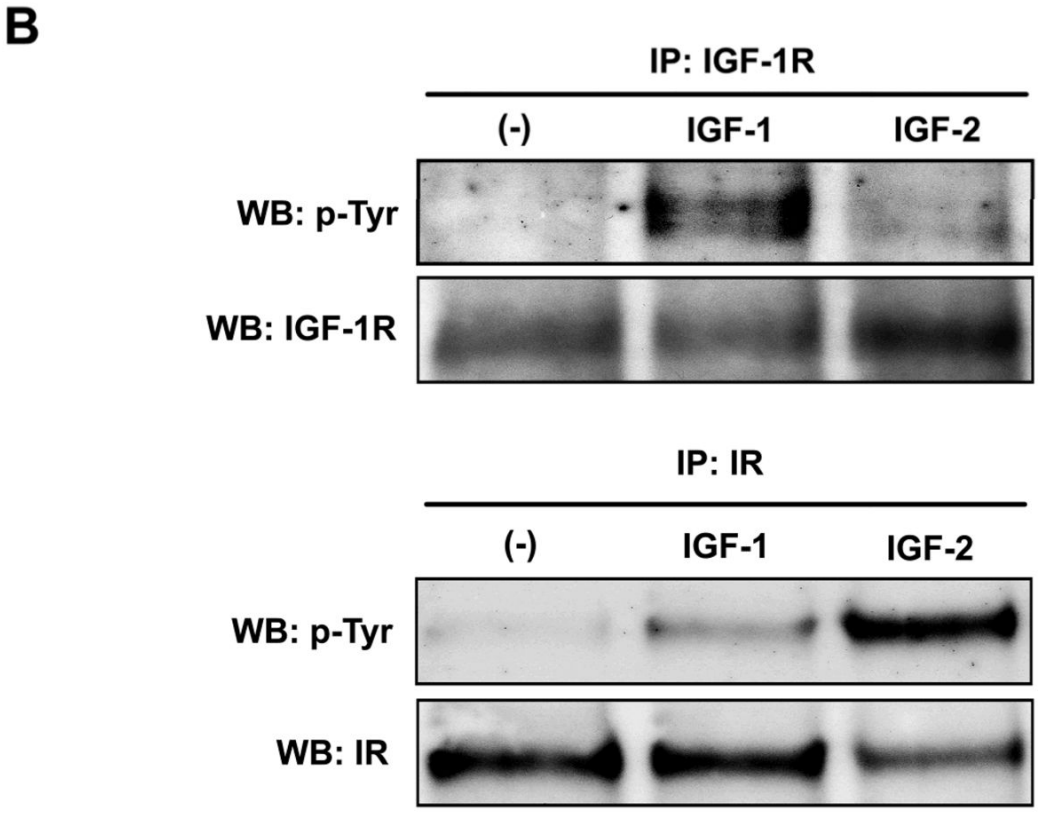

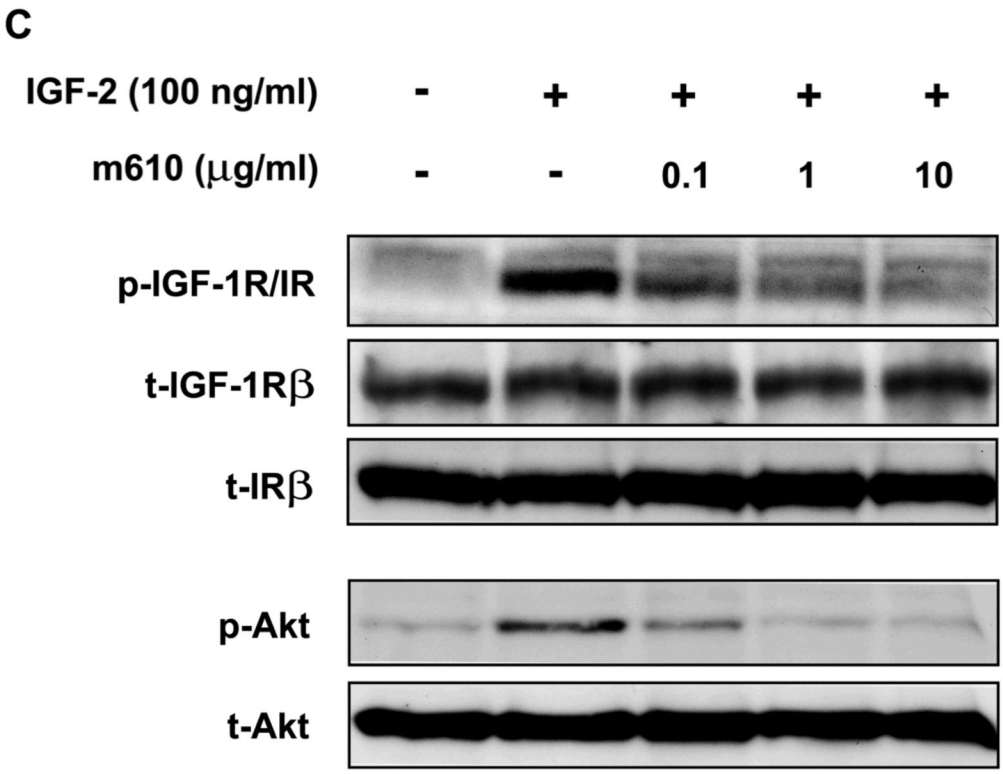

Fig. 6. M610 inhibits IGF-2-induced cell proliferation and phosphorylations of IGF-1R/IR and Akt in MDA PCa 2b cells

A, MDA PCa 2b cells were treated for 48 hours with serum-free medium alone, with various concentrations of IGF-2, with the control antibody plus 100 ng/mL of IGF-2, or with various concentrations of m610 in the presence or absence of 100 ng/mL of IGF-2. The cells were counted using trypan blue dye exclusion. Data are the means of triplicate determinations and are representative of three independent experiments; bars, ± SE. $^{\#}P < 0.05$, compared with serum-free medium. $^{**}P < 0.01$, compared with control antibody group. **B**, The cells were treated with 100 ng/ml of IGF-1 or IGF-2. Tyrosine phosphorylation of immunoprecipitated IGF-1R or IR were examined by a western blot analysis. WB, western blot; IP, immunoprecipitation; p-Tyr, phosphorylated tyrosine. **C,** The cells were pre-incubated with the indicated concentrations of m610, and 100 ng/mL of IGF-2 was added. IGF-1R/IR and Akt phosphorylation levels and the total protein levels in the lysates were examined by western blot analysis. p-, phosphorylated; t-, total.